J Mater Sci (2009) 44:3376–3381
DOI 10.1007/s10853-009-3441-8

Effect of Ag on the electrical properties of a-$Ge_{20}Se_{80}$ glasses

**Gurinder Singh · N. Goyal · G. S. S. Saini ·
P. S. Chandel · S. K. Tripathi**

Received: 18 March 2008 / Accepted: 24 March 2009 / Published online: 24 April 2009

Abstract This article reports the effect of Ag impurity (low ~4 and ~6 at.% and high ~10 at.%) on the ac conductivity (σ_{ac}) of a-$Ge_{20}Se_{80}$ glass. Frequency (ω)-dependent ac conductance and capacitance of the samples over a frequency range ~100 Hz to 50 kHz was taken in the temperature range ~268–358 K. At frequency 2 kHz and temperature 298 K, the value of σ_{ac} increases at low as well as at higher concentration of Ag. The σ_{ac} is proportional to ω^s for undoped and doped samples. The value of frequency exponent (s) decreases as the temperature increases.

Introduction

Chalcogenide glasses have received a lot of attention because of their potential use in various solid-state devices. They have been attracting much attention in the field of electronics as well as in infrared optics, since they exhibit several peculiar phenomena useful for devices such as electrical switches, memories, image storage, and photoresistors. Studies of the electronic nature of amorphous materials provide information about its electrical behavior and this may be related to structural properties. The common feature of these glasses is the presence of localized states in the mobility gap, as the result of the absence of the long-range order as well as various inherent defects. The disorder in atomic configuration is responsible for the existence of localized electronic states within the material. Because the charge carriers are localized, ac technique is often employed to probe their behavior.

Selenium (Ge–Se) glassy system exhibits properties, which are unusual, and possibly unique, relative to other semiconductors. Ge_xSe_{100-x} is being actively investigated as high-efficiency semiconductors for holographic recording, reversible phase change optical recording media and memory devices, and solar energy conversion applications [1–3]. The physical properties of these glasses are influenced by the presence of inherent defects. These inherent defects in chalcogenide glasses originate due to the rearrangements taking place at the prevalent chain ends (D^+- and D^--charged dangling bonds or $C_3{}^+$ and $C_1{}^-$ intimate valence–alternation pair, IVAP) [4, 5].

The interest in superionic glasses has increased considerably in recent years because of the potential application of these materials in different fields [6–8]. Glasses on the selenium-rich side of the Ge–Se–Ag system are fast ionic conductors with silver as the mobile cation. Although several studies have been undertaken on Ag-doped chalcogenide glasses, especially on Ge–Se–Ag systems [9–11], GeSeAg glassy system share many structure and transport characteristics with the (network former)-(network modifier) family of glasses. In this glass, Ge is termed as the network forming cation, Ag as the mobile cation, and Se as the anion [9]. The structure of this glass has been investigated by many authors [12–14], and a short range order due to $GeSe_{4/2}$ tetrahedra was reported. However, the correlation of the Ag is motive of controversy. The glass homogeneity generates dispute too. Some works propose that $(Ge_{0.25}Se_{0.75})_{0.75}Ag_{0.25}$ glasses are homogeneous bulk glasses [12, 13]. However, in a recent work, ternary $(Ge_zSe_{1-z})_{1-y}Ag_y$ bulk glasses in the Se-rich region ($z < 1/3$) are shown to be intrinsically phase separated into an

---

G. Singh · N. Goyal · G. S. S. Saini · P. S. Chandel ·
S. K. Tripathi (✉)
Centre of Advanced Study in Physics, Panjab University,
Chandigarh 160 014, India
e-mail: surya@pu.ac.in; surya_tr@yahoo.com

Ag_2Se-rich glass and a residual Ge_tSe_{1-t} ($t > z$ at $y \neq 0$) with Ag acting as network modifier [15]. Mitkova et al. observed bimodal glass transition temperatures. In contrast, Ge-rich glasses ($z > 5/2$) were reported as homogeneous, wherein Ag acts as a network former, replacing available Ge sites of the backbone to be threefold coordinated to Se.

This article reports the temperature- and frequency-dependent σ_{ac} of $(Ge_{20}Se_{80})_{100-x}Ag_x$ glassy alloys. The results reported in this study provide information about the effect of Ag alloying in $Ge_{20}Se_{80}$ glass. The modified correlated barrier hopping (CBH) model [16, 17] has been used to explain the effect of Ag doping. The second describes the experimental details. The results have been presented and discussed in third section. The last section deals with the conclusion of this work.

Experimental

$(Ge_{20}Se_{80})_{100-x}Ag_x$ ($x = 0$, 4, 6, and 10 at.%) glassy materials have been prepared by taking the constituent elements (M/s Alfa Aesar, USA; purity ~99.999%) in required atomic weight percentages. The materials were mixed together and sealed in quartz ampoules (length ~10 cm, diameter ~1 cm) under a pressure of ~1.33×10^{-5} mbar. These ampoules were mounted in a furnace for heating. Initially, the temperature of the furnace was raised slowly and kept constant at the melting temperature of each constituent element (1234 K for Ag, 490 K for Se, and 1210 K for Ge) for about 2 h each. The temperature was then raised and maintained at about 50 K more than the highest melting point of the constituents (1284 K) for about 24 h. The ampoules were immediately cooled in liquid nitrogen for the materials to go into the glassy state. The glassy materials, in the form of ingots, were obtained by breaking the ampoules. To verify the amorphous nature of these glasses, X-ray diffraction (XRD) study on all samples was done (Philips X-Ray Generator, Model: PW1729 along with a PW1710 Diffractometer). No peaks have been observed for the materials prepared by the above-mentioned technique, thereby confirming the amorphous nature of the prepared materials.

Compressed pellets (diameter: 0.687 cm; thickness: 1–2 mm) were prepared by grinding the bulk ingots into fine powder and compressing the resulting powder in a die under a hydraulic press (pressure ~10^6 kg/m^2). While making compressed pellets, one must ensure that the powder is compressed to maximum compaction so that there were no voids in the sample. A three-terminal sample holder has been fabricated for the measurement of σ_{ac} of the pellet-shaped samples. Provision was made for measuring the vacuum inside the sample holder. Cylindrical brass jacket was used as outer cover to provide excellent electromagnetic shielding. A built-in micrometer was used for the measurement of sample thickness. Temperature of the sample was noted with the help of a thermocouple which was kept close to the sample. A low-temperature bath (Julabo F-70 VC/K) was used for controlling the temperature of the samples. Vacuum pumping system (Model: VS-65D, H.H.V., India) was used to achieve a vacuum up to ~1.33×10^{-5} mbar inside the sample holder. Aquadag emulsion is used to make electrical contacts for the pellets. A General Radio Bridge (Model: 1615-A) was used for the measurements of frequency-dependent σ_{ac}. The bridge consists of an audio oscillator (Model: 1311), a tuned amplifier (Model: 1232-A), and a null detector, which permits balance to a resolution of one part in a million.

Results and discussion

Figure 1a–d shows the frequency dependence of measured conductivity (σ_{ac}) for the undoped $Ge_{20}Se_{80}$ and doped $(Ge_{20}Se_{80})_{96}Ag_4$, $(Ge_{20}Se_{80})_{94}Ag_6$, and $(Ge_{20}Se_{80})_{90}Ag_{10}$ samples at different temperatures. The conductivity data presented in these figures can be fitted with the relation $\sigma_{ac} = A\omega^s$, where s is the frequency exponent and A is a constant. The decrease in slope with increasing temperature indicates that the value of s decreases with increasing temperature. Figure 2a–c shows the temperature dependence of σ_{ac} of $Ge_{20}Se_{80}$, $(Ge_{20}Se_{80})_{96}Ag_4$, $(Ge_{20}Se_{80})_{94}Ag_6$, and $(Ge_{20}Se_{80})_{90}Ag_{10}$ glasses at frequencies 2, 10, and 20 kHz, respectively. From the figures, it is clear that the conductivity increases with temperature more in the case of pure sample. Whereas, in case of lower and higher doping of Ag ($x = 4$, 6, and 10 at.%), the increase in conductivity is small with temperature. However, a large increase in conductivity has been observed at higher Ag ($x = 10$ at.%) concentration at all temperatures. Figure 3 shows the temperature dependence of the frequency exponent s for all the four samples. It is clear from the figure that the value of s decreases with the increase in temperature as well as with the increase in Ag concentration. This decrease is more in case of higher Ag (10 at.%) doping concentrations as compared to the lower Ag concentrations. Figure 4 shows the graph between natural log of dielectric loss (ε'') versus natural log of frequency (Nyquist plots) of a-$Ge_{20}Se_{80}$ glassy alloy at different temperatures. It is clear from the figure that the value of dielectric loss decreases with frequency at all temperatures and increases with temperature at a particular frequency. The similar results have been obtained for other GeSeAg samples (results not shown here).

Fig. 1 Frequency dependence of conductivity at different temperatures in (**a**) a-$Ge_{20}Se_{80}$, (**b**) a-$(Ge_{20}Se_{80})_{96}Ag_4$, (**c**) a-$(Ge_{20}Se_{80})_{94}Ag_6$, and (**d**) a-$(Ge_{20}Se_{80})_{90}Ag_{10}$ alloys

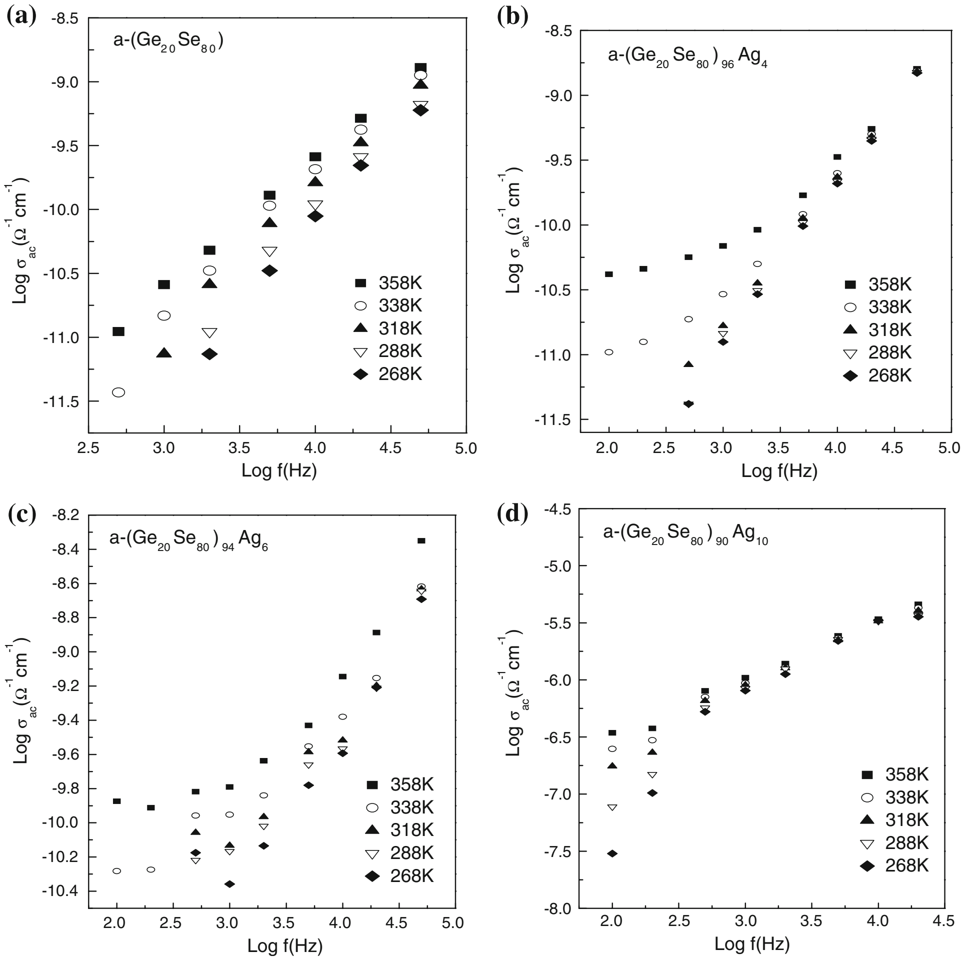

Using a modified CBH model [16, 17], the above results can be explained as discussed below. According to this model:

$$\sigma_{ac} = \frac{n\pi^3}{24} N^2 \omega \varepsilon \varepsilon_0 R_\omega^6 \quad (1)$$

where n is the number of polaron involved in the hopping process, ω is the frequency, ε is the permittivity, and R_ω is the hopping distance for the condition $\omega\tau = 1$, and is given by [16]:

$$R_\omega = \frac{ne^2}{\pi\varepsilon\varepsilon_0\{W_M + kT\ln(\omega\tau_0)\}} \quad (2)$$

The value of frequency exponent s is calculated from Eqs. 2 and 3, and is equal to:

$$s = \frac{d(\ln\sigma_{ac})}{d(\ln\omega)} = 1 - \frac{6kT}{W - kT\ln[1/\omega\tau_0]} \quad (3)$$

where

$$NN_P = N_T^2 \quad \text{(For bipolaron hopping)} \quad (4)$$

where N is the concentration of localized sites, N_P is the concentration of carriers, and N_T is the number of density of states.

$$NN_P = N_T^2\exp(-U_{eff}/2kT) \quad \text{(For single polaron hopping)} \quad (5)$$

where U_{eff} is the effective correlation energy.

Total conductivity is the combined mechanism of these processes. These processes are bipolaron hopping between D^+ and D^- centers and single polaron hopping between D^0 and D^- centers and D^0 and D^+ centers. Here, W is equal to W_M, which is slightly less than the band gap for the bipolaron hopping. However, it is equal to W_1 and W_2 for the two types of single polaron hopping mechanisms, which are substantially less than W_M for bipolaron hopping. The smaller values of W_1 and W_2 for single polaron hopping means that the value of R_w is much greater for single polaron hopping as compared to bipolaron hopping described by Eq. 2.

The structure of Ag–Ge–Se glasses has been investigated by X-ray diffraction [18], neutron diffraction [13], neutron inelastic and Raman scattering [19, 20], EXAFS [21], and differential anomalous X-ray scattering (DAS) [12]. The structure of the glass corresponding to a stoichiometric composition $GeSe_2$ was thoroughly investigated and was concluded to be formed by tetrahedral $GeSe_4$ connected by

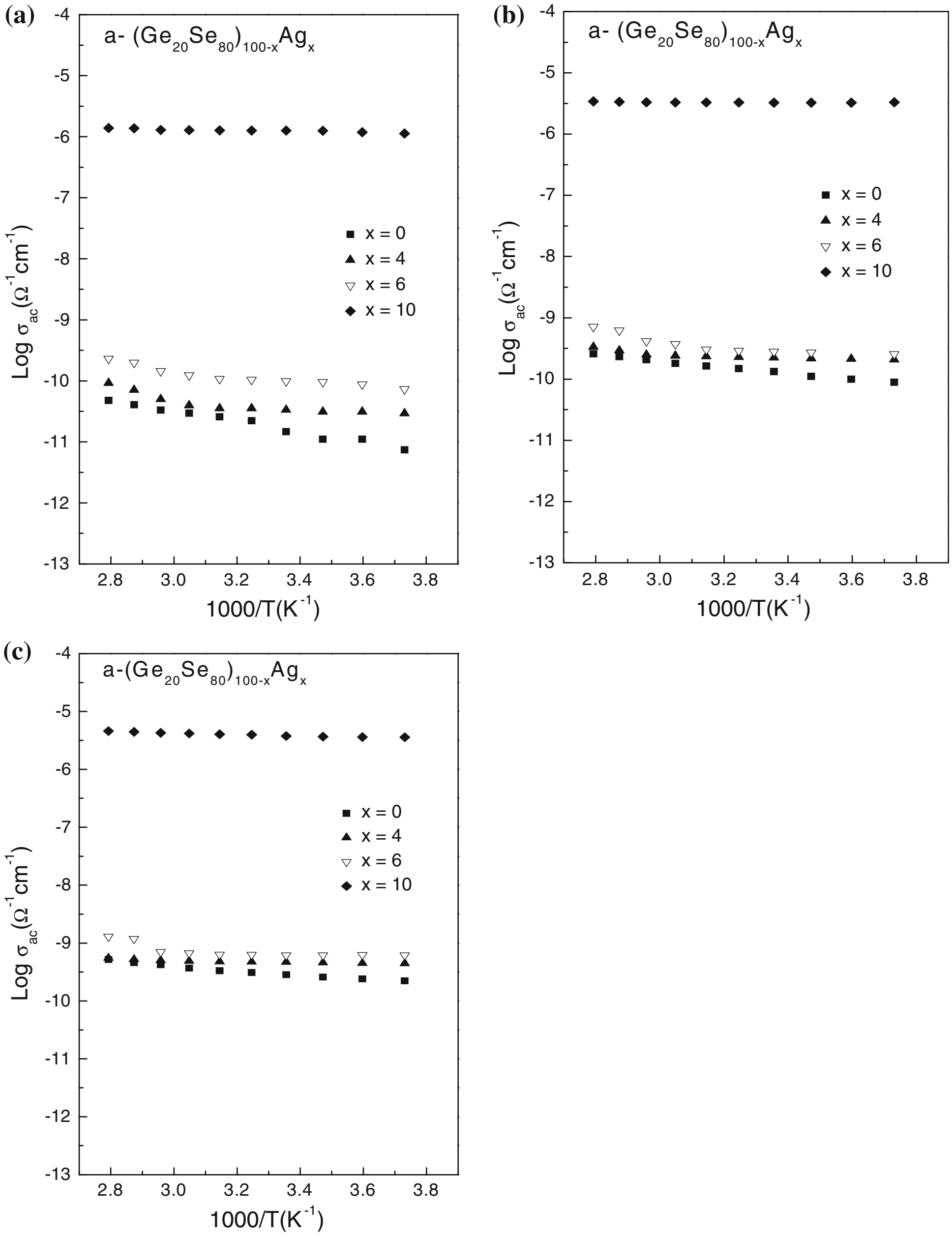

Fig. 2 Temperature dependence of ac conductivity at (**a**) 2 kHz, (**b**) 10 kHz, and (**c**) 20 kHz

edge and corner sharing [22, 23] to construct quasi-two-dimensional distorted layers, which is in good agreement with the outrigger-raft structure model [24]. The structure of $GeSe_3$ glass is formed of similar $GeSe_4$ units as in $GeSe_2$ glass and excess Se–Se connections. The excess selenium creates short chain or screw type of $(–Se–)_n$ and also causes the depolymerization of the layered network of $GeSe_4$ tetrahedra. Unusual changes in ionic conductivity of silver in this study suggest a structural change around silver ions in the glasses.

A sharp transition from semiconductor to superionic conductor in $(Ge_{20}Se_{80})_{100-x}Ag_x$ glasses has been detected by the author. This is evident from Fig. 2a–c where sharp increase in conductivity for $x = 10$ at.% has been reported. A percolation transition at $x = 10$ is obtained by Kawasaki et al. [25]. This phenomenon of percolation could be explained for the systems of GeSeAg glasses. They studied the electrical properties of $Ag_x(GeSe_3)_{1-x}$ $(0 \leq x \leq 0.571)$ glasses and investigated the impedance spectra and electric motive force of these samples. They found that as the concentration of silver is increased, the total electrical conductivity increases from 10^{-14} to 10^{-3} S/cm at about $x = 0.3$. This rapid increase is chiefly due to an appearance of silver ion migration. Armand et al. [26] suggested that glasses GeXAg (X = S, Se) containing small amounts of Ag_2X have an inhomogeneous structure composed of Ag_2X clusters embedded in a GeX_2 network, which becomes homogeneous at higher concentration of Ag_2X. Therefore, when the Ag content is low, the clusters do not connect

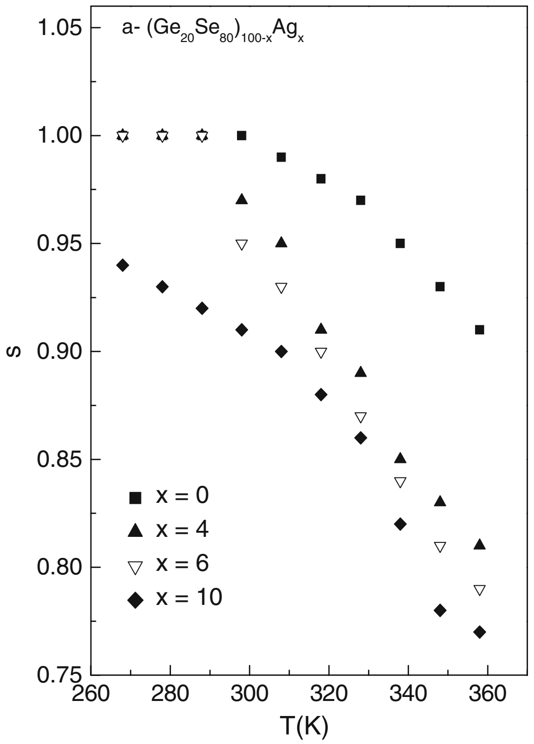

Fig. 3 Variation of frequency exponent s with temperature

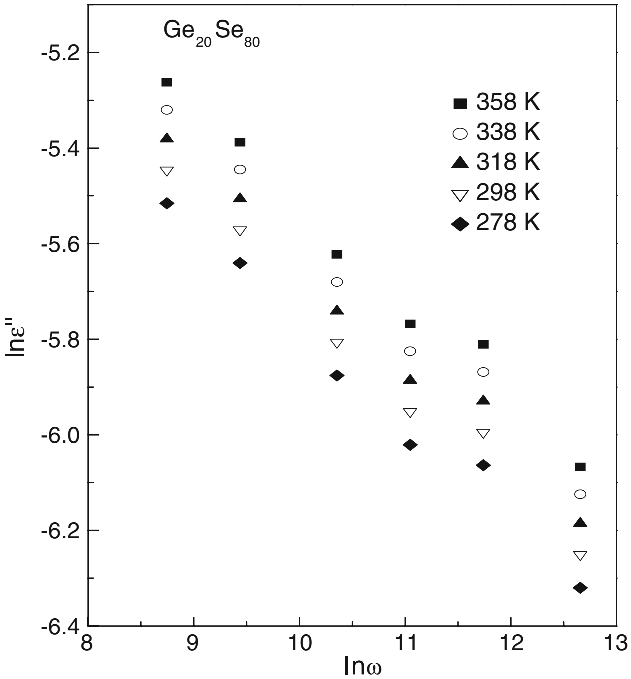

Fig. 4 Variation of ln ε'' vs. ln ω at different temperatures

themselves and the sample does not conduct Ag^+ ions. However, when the Ag content increases to $x = 10$ at.%, the clusters Ag_2X connect themselves or the amorphous structure become homogeneous and the sample turns into ionic conductor as reported by the Mirandou et al. [27] in the $(Ge_{25}Se_{75})_{100-x}Ag_x$ glasses at about $x = 10$. Pattanayak and Asokan [28] have shown that $Ge_{0.15}Se_{0.85-x}Ag_x$ glasses are microscopically phase separated and composed of Ag_2Se clusters and $GeSe_2$–Se network. When Ag concentration exceeds 10%, the Ag_2Se clusters embedded in the $GeSe_2$–Se network percolates. The signature of this percolation threshold is observed in the sudden appearance of two exothermic crystallization peaks in ADSC runs. Borisova et al. [29] studied the glass-forming ability of the $(Ge_{0.25}Se_{0.75})_{100-x}Ag_x$ ternary system by water quenching. They found that in samples with composition $Ge_{25}Se_{75}$, the vitreous behavior could be retained by introducing a maximum Ag content of 30 at.%. Ribes and co-workers [30] reported very extensive data on the electrical data as well as diffusion coefficient of silver in similar chalcogenide glasses. They observed a discontinuous variation of the transport properties of silver ions in Ag–Ge–S and Ag–Ge–Se–Sb glasses and concluded that the ionic transport mechanism in low concentration of silver (<5 at.%) is different from that in higher concentration (>10 at.%). Piarristeguy et al. [31] have carried out the field effect-scanning electron microscopy (FE-SEM) and electric force microscopy (EFM) measurements on bulk Ag_2S–As_2S_3 glasses with different silver concentrations. They indicated that the glass $Ag_{1.2}$ is on the whole homogeneous, whereas the Ag_4 and $Ag_{9.8}$ glasses are phase separated. For Ag_4 glass, the silver-rich phase corresponds to nodules of 200–350 nm embedded in a connecting silver-poor phase. For $Ag_{9.8}$, the silver-rich phase is the connecting phase, whereas the silver-poor phase corresponds to nodules of 250–700 nm. Two conductivity regimes are observed by Pradel et al. [32] during the study of ion transport and structure of Ag-rich chalcogenide glasses. They have observed that the change from the low-conductivity regime to the high-conductivity regime in the phase-separated glasses Ag_2S–GeS_2 and Ag_2S–As_2S_3 occurs when the regions containing the Ag-rich phase start to connect. This behavior is characteristic of a percolation threshold with the Ag-poor phase (Ag-rich phase) being responsible for the conductivity at low silver (high silver) content. Wagner et al. [33] have studied the optically and thermally induced diffusion of silver and its diffusion profiles in amorphous layers of Ge–Se systems. They have shown that the diffusion is of a bipolar character and its rate is controlled by the transport of low-mobility holes. Diffusion rates are much higher on conductive than on nonconductive substrates.

Conclusions

Electrical conductivity measurements have been taken in undoped $Ge_{20}Se_{80}$ and doped with Ag (low and high concentrations) metal. Frequency-dependent σ_{ac} measurements at different temperatures show that the value of σ_{ac}

increases with the doping of Ag. The value of *s* decreases at all concentrations at high temperature. It is observed that the addition of Ag increases the conductivity of GeSeAg glassy system. This is because when the Ag content increases, the clusters Ag_2X connect themselves or the amorphous structure becomes homogeneous and the sample turns into an ionic conductor.

Acknowledgement This work was financially supported by the C.S.I.R. (major project), New Delhi.

References

1. Calvez L, Ma HL, Lucas J, Zhang XH (2007) Adv Mater 19:129
2. Calvez L, Lucas P, Roze M, Ma HL, Lucas J, Zhang XH (2007) J Appl Phys A 89:183
3. Nemcsics A, Kovacs S, Labadi Z, Hesse KF, Czank M, Turmezei P, Motrya S (2005) Solar Energy Mater Solar Cells 89:175
4. Street RA, Mott NF (1975) Phys Rev Lett 35:1293
5. Kastner M, Adler D, Fritzsche H (1976) Phys Rev Lett 37:1504
6. Frumar M, Wagner T (2003) Curr Opin Solid State Mater Sci 7:117
7. Boolchand P, Bresser WJ (2001) Nature 410:1070
8. Bunde A, Funke K, Ingram MD (1998) Solid State Ionics 1:105
9. Urena MA, Fontana M, Arcondo B, Clavaguera-Mora MT (2003) J Non-Cryst Solids 151:320
10. Wang Y et al (2003) J Phys Condens Matter 15:S1573
11. Dejus RJ et al (1992) J Non-Cryst Solids 143:162
12. Westwood JD, Gergopoulos P, Whitmore DH (1988) J Non-Cryst Solids 107:88
13. Dejus RJ, Susman S, Volin K, Montague D, Price D (1992) J Non-Cryst Solids 143:162
14. Piarristeguy A, Mirandou M, Fontana M, Arcondo B (2000) J Non-Cryst Solids 273:30
15. Mitkova M, Wang Y, Boolchand P (1999) Phys Rev Lett 83:3848
16. Shimakawa K (1982) Philos Mag B 46:123
17. Shimakawa K (1983) Philos Mag B 48:778
18. Bourne LC, Rowland SC, Bienenstock A (1981) J Phys Colloque C4:951
19. Dejus RJ, Lepoire DJ, Susman S, Volin K, Price DL (1991) Phys Rev B Condens Matter 44:11705
20. Dejus RJ, Lepoire DJ, Price DL, Susman S, Volin K (1989) J Non-Cryst Solids 114:37
21. Ibanez A, Armand P, Philippot E, Dexpert H (1993) Solid State Ionics 59:157
22. Peyroutou C, Peytavin S, Ribes M, Dexpert H (1989) J Solid State Chem 82:70
23. Walter U, Price DL, Susman S, Volin KJ (1988) Phys Rev B 37:4232
24. Kumagai N, Shirafuji J, Inuishi Y (1977) J Phys Soc Jpn 42:1261
25. Kawasaki M, Kawamura J, Nakamura Y, Aniya M (1999) Solid State Ionics 123:259
26. Armand P, Ibanez A, Dexpert H, Bittencourt D, Raoux D, Philippot E (1992) J Phys IV Colloque C22:2
27. Mirandou M, Fontana M, Arcondo B (2003) J Mater Process Technol 143–144:420
28. Pattanayak P, Asokan S (2005) J Appl Phys 97:013515
29. Borisova ZU, Rykova TS, Turkina EYu, Tabolin AR (1984) Izv Akad Nauk SSR Neorg Mater 20:1796
30. Bychkov E, Tsegelink V, Vlasov Y, Pradel A, Ribes M (1996) J Non-Cryst Solids 208:1
31. Piarristeguy A, Ramonda M, Kuwata N, Pradel A, Ribes M (2006) Solid State Ionics 177:3157
32. Pradel A, Kuwata N, Ribes M (2003) J Phys Condens Matter 15:S1561
33. Wagner T, Jilkova R, Frumer M, Vlcek M (1994) Int J Electron 77:185